

Pulsed Optics

C. Hirlimann

With 23 Figures

2.1 Introduction

Optics is the field of physics which comprises knowledge on the interaction between light and matter. When the superposition principle can be applied to electromagnetic waves or when the properties of matter do not depend on the intensity of light, one speaks of linear optics. This situation occurs with regular light sources such as light bulbs, low-intensity light-emitting diodes and the sun. With such low-intensity sources the reaction of matter to light can be characterized by a set of parameters such as the index of refraction, the absorption and reflection coefficients and the orientation of the medium with respect to the polarization of the light. These parameters depend only on the nature of the medium. The situation changed dramatically after the development of lasers in the early sixties, which allowed the generation of light intensities larger than a kilowatt per square centimeter. Actual large-scale short-pulse lasers can generate peak powers in the petawatt regime. In that large-intensity regime the optical parameters of a material become functions of the intensity of the impinging light. In 1818 Fresnel wrote a letter to the French Academy of Sciences in which he noted that the proportionality between the vibration of the light and the subsequent vibration of matter was only true because no high intensities were available. The intensity dependence of the material response is what usually defines nonlinear optics. This distinction between the linear and nonlinear regimes clearly shows up in the polynomial expansion of the macroscopic polarization of a medium when it is illuminated with an electric field \mathbf{E} :

$$\begin{aligned}
 \frac{\mathbf{P}}{\varepsilon_0} = & \chi^{(1)} \cdot \mathbf{E} && \text{Linear optics, index, absorption} \\
 & + \chi^{(2)} : \mathbf{E}\mathbf{E} && \text{Nonlinear optics, second-harmonic} \\
 & && \text{generation, parametric effects} \\
 & + \chi^{(3)} : \mathbf{E}\mathbf{E}\mathbf{E} && \text{third-harmonic generation, nonlinear} \\
 & && \text{index} \\
 & + \dots
 \end{aligned} \tag{2.1}$$

In this expansion, the linear first-order term in the electric field describes linear optics, while the nonlinear higher-order terms account for nonlinear optical effects (ε_0 is the electric permittivity).

The development of ultrashort light pulses has led to the emergence of a new class of phase effects taking place during the propagation of these pulses through a material medium or an optical device. These effects are mostly related to the wide spectral bandwidth of short light pulses, which are affected by the wavelength dispersion of the linear index of refraction. Their analytical description requires the Taylor expansion of the light propagation factor k as a function of the angular frequency ω ,

$$k(\omega) = k(\omega_0) + k'(\omega - \omega_0) + \frac{1}{2}k''(\omega - \omega_0)^2 + \dots \quad (2.2)$$

Contrary to what happens in “classical” nonlinear optics, these nonlinear effects occur for an arbitrarily low light intensity, provided one is dealing with short (< 100 fs) light pulses. Both classes of optical effects can be classified under the more general title of “pulsed optics.”

2.2 Linear Optics

2.2.1 Light

If one varies either a magnetic or an electric field at some point in space, an electromagnetic wave propagates from that point, which can be completely determined by Maxwell’s equations.

If the magnetic field has an amplitude which is negligible when compared to the electric field, the propagation equation for light can be written as

$$\nabla^2 \mathbf{E} = \frac{1}{c^2} \frac{\partial^2 \mathbf{E}}{\partial t^2}, \quad \frac{1}{c^2} = \mu_0 \varepsilon_0, \quad (2.3)$$

where c is a parameter, usually called the velocity of light, depending on the electric and the magnetic permittivity, ε_0 and μ_0 respectively, of the material medium in which the wave is propagating. Equation 2.3 is a second-order differential equation, for which retarded plane waves are the simplest propagating solutions,

$$E_y = \text{Re} \left(E_0 e^{i\omega(t-x/c)} \right). \quad (2.4)$$

This particular solution 2.4 describes the propagation of a transverse electric field E_y along the positive x axis. The amplitude of the electric field varies periodically as a cosine function in time with angular frequency ω and in space with wavelength $\lambda = 2\pi c/\omega$. At any given point x along the propagation axis the amplitude has the same value as it had at the earlier time $t - x/c$, when it was at the origin ($x = 0$).

A rewriting of 2.4 as

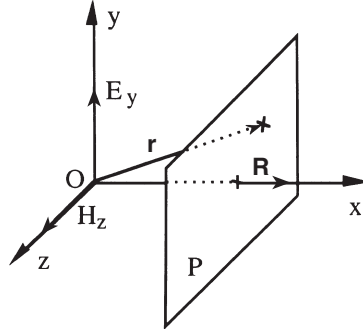


Fig. 2.1. Plane-wave propagation

$$E_y = \text{Re} \left(E_0 e^{i(\omega t - \mathbf{k} \cdot \mathbf{r})} \right), \quad |\mathbf{k}| = \frac{\omega}{c} = \frac{2\pi}{\lambda}, \quad (2.5)$$

allows the introduction of the wave vector \mathbf{k} of the light. Figure 2.1 shows the geometry of the propagation of a plane wave. Let us consider the plane P orthogonal to the propagation vector \mathbf{k} , at distance x from the origin O . For any point in this plane, at distance r from the origin O , the scalar product $\mathbf{k} \cdot \mathbf{r} = kx = \omega x/c$ is constant; therefore, at a given time t , plane P is a plane of equal phase or equal time delay for a plane wave. A plane wave with a wavelength in the visible range ($400 > \lambda > 800 \text{ nm}$) has an angular frequency ω equal to a few petahertz.

It is to be noticed that a plane wave, being a simple sine or cosine function, has an infinite duration and its spectrum, which contains only one angular frequency ω , is a δ distribution. A plane wave is the absolute opposite of a light pulse!

Up to this point light has been considered as a wave, but its particle behavior cannot be ignored. The wave-particle duality has the following meaning. The wave description of light is continuous in both time and space, while the particle description is discrete. In our classical culture these two visions are antithetical and one cannot be reduced to the other. Nowadays physics says and experiments show that light is both continuous and discrete. In the particle description light is made of photons, energy packets equal to the product of the frequency and Planck's constant $h\nu = \hbar\omega$. Photons have never been observed at rest and as they travel at the speed of light, relativity implies that their mass would be zero.

Fermat's principle states that the path of a ray propagating between two fixed point, A and B must be a stationary path, which in a mathematical point of view translates as

$$\delta \int \mathbf{k} \cdot d\mathbf{l} = 0, \quad (2.6)$$

δ standing for a variation of the path integral and $d\mathbf{l}$ for an elementary path element anywhere between A and B.

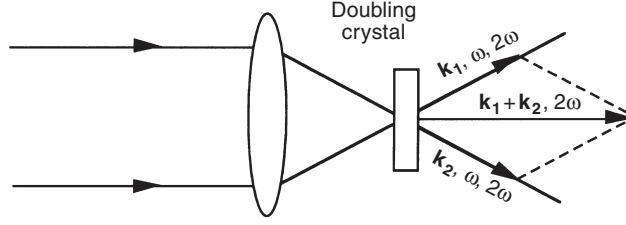


Fig. 2.2. Energy and momentum conservation in the doubling geometry used to record background-free autocorrelation traces of short optical pulses. Both the energy and the momentum are conserved during the mixing process

The path of the light is either the fastest one or the slowest one (in the latter some cases of reflection geometry with concave mirrors).

For a material particle with momentum \mathbf{p} , Maupertuis's principle states that the integrated action of the particle between two fixed points A and B must be a minimum, which translates as

$$\delta \int \mathbf{p} \cdot d\mathbf{l} = 0. \quad (2.7)$$

By analogy, the wave vector \mathbf{k} for the light can be seen as the momentum of a zero-mass particle travelling along the light rays.

When light interacts with matter, both the energy and the momentum are conserved quantities. As an example, let us consider the dual-beam frequency-doubling process used in the background-free autocorrelation technique (Fig. 2.2).

In this geometry, two beams are incident, at an angle α , on a doubling crystal that can mix two photons with angular frequency ω and momenta \mathbf{k}_1 and \mathbf{k}_2 , and produce one photon with angular frequency ω_2 and momentum \mathbf{k} . Energy conservation implies that $\omega_2 = 2\omega$, while momentum conservation yields $\mathbf{k} = \mathbf{k}_1 + \mathbf{k}_2$, $\mathbf{k} = 2\mathbf{k}_1$ or $\mathbf{k} = 2\mathbf{k}_2$. Five rays therefore exit the doubling material: two rays are at the fundamental frequency ω in the directions \mathbf{k}_1 and \mathbf{k}_2 of the incident rays, and superimposed on them are two rays with doubled frequency 2ω and momentum vectors $2\mathbf{k}_1$ and $2\mathbf{k}_2$. The fifth ray, with angular frequency 2ω , is oriented along the bisector of the angle α , corresponding to the geometrical sum $\mathbf{k}_1 + \mathbf{k}_2$.

2.2.2 Light Pulses

It is quite easy to produce “gedanken” light pulses. Let us start with a monochromatic plane wave, previously defined as (Fig. 2.3)

$$E_y = \text{Re} (E_0 e^{i\omega_0 t}). \quad (2.8)$$

The time representation of the field is an unlimited cosine function. Constructing a light pulse implies multiplying 2.8 by a bell-shaped function. To

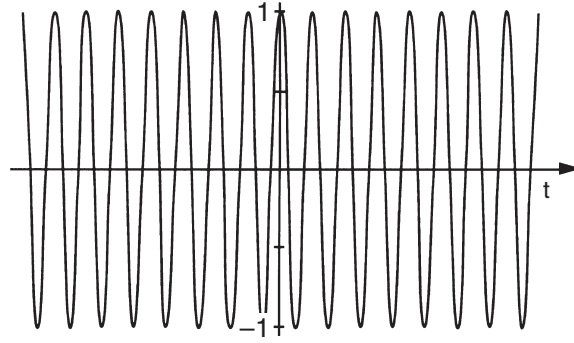


Fig. 2.3. Schematic time evolution of the electric field of a monochromatic plane wave. Notice that because of the finite width of the figure this picture is already representative of a light pulse having a rectangular envelope

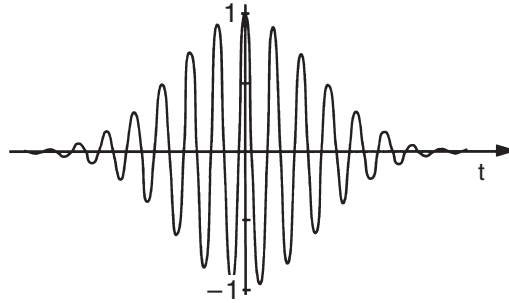


Fig. 2.4. Time evolution of the electric field in a Gaussian-shaped pulse. This pulse is built up by multiplying a cosine function by a Gaussian envelope function

simplify further calculation, we choose to multiply by a Gaussian function. A Gaussian pulse can be written

$$E_y = \text{Re} \left(E_0 e^{(-\Gamma t^2 + i\omega_0 t)} \right) \quad (2.9)$$

and its time evolution is shown in Fig. 2.4.

Γ is the shape factor of the Gaussian envelope; it is proportional to the inverse of the squared duration t_0 , i.e. $\Gamma \propto t_0^{-2}$.

Let us now turn to the spectral content of a light pulse. This can be obtained by calculating the modulus of the Fourier transform of the time evolution function of the pulse. As said earlier, a plane wave oscillates with the unique angular frequency ω_0 and its Fourier transform is a Dirac distribution $\delta(\omega_0)$ (Fig. 2.5).

The Fourier transform of a Gaussian pulse is also a Gaussian function (Fig. 2.6). Therefore the frequency content of a light pulse is larger than the

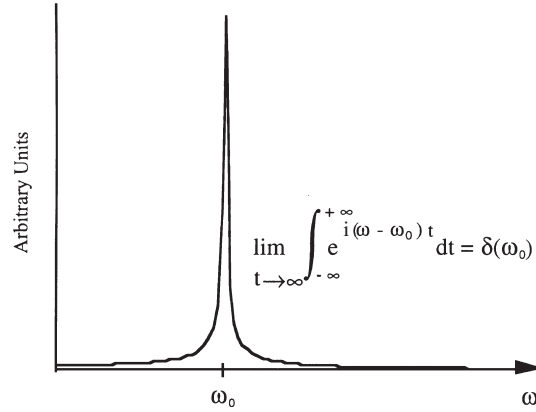


Fig. 2.5. Numerical Fourier transform of the truncated cosine function shown in Fig. 2.3. As the width of the cosine function grows larger and larger ($t_0 \rightarrow \infty$), the Fourier transform tends toward a Dirac distribution $\delta(\omega_0)$ with zero width

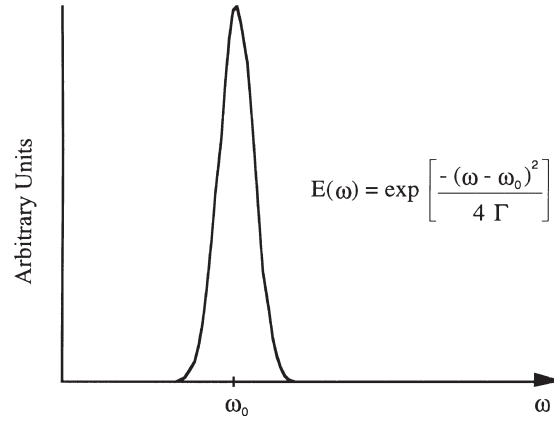


Fig. 2.6. Numerical Fourier transform of the Gaussian pulse shown in Fig. 2.4. The transformed function is also a Gaussian function with a frequency width proportional to Γ

unique frequency of a plane wave. The mathematical expression for the spectrum is given in Fig. 2.6 and the width of the spectrum is proportional to Γ .

2.2.3 Relationship Between Duration and Spectral Width

We have just empirically observed that the spectral width and the duration of a pulse are related quantities. What is the exact relationship? We start from the general time and frequency Fourier transforms of a pulse:

$$\varepsilon(t) = \frac{1}{2\pi} \int_{-\infty}^{+\infty} E(\omega) e^{-i\omega t} d\omega, \quad E(\omega) = \int_{-\infty}^{+\infty} \varepsilon(t) e^{i\omega t} dt. \quad (2.10)$$

When the duration and the spectral width of the pulse are calculated using the standard statistical definitions

$$\begin{aligned} \langle \Delta t \rangle &= \frac{\int_{-\infty}^{+\infty} t |\varepsilon(t)|^2 dt}{\int_{-\infty}^{+\infty} |\varepsilon(t)|^2 dt}, \\ \langle \Delta \omega^2 \rangle &= \frac{\int_{-\infty}^{+\infty} \omega^2 |E(\omega)|^2 d\omega}{\int_{-\infty}^{+\infty} |E(\omega)|^2 d\omega}, \end{aligned} \quad (2.11)$$

it can be shown that these quantities are related through the following universal inequality:

$$\Delta t \Delta \omega \geq \frac{1}{2}. \quad (2.12)$$

This classical-physics relationship, which leads to the quantum-mechanical time–energy uncertainty principle, has several important consequences in the field of ultrashort light pulses.

- In order to produce a light pulse with a given duration it is necessary to use a broad enough spectral bandwidth. A Gaussian-shaped pulse lasting for one picosecond (10^{-12} s) has a minimum spectral bandwidth of 441 MHz ($\Delta\omega = 4.41 \times 10^{11}$ Hz). If the central frequency ν_0 of the pulse lies in the visible part of the electromagnetic spectrum, say $\nu_0 = 4.84 \times 10^{14}$ Hz (wavelength $\lambda_0 = 620$ nm), then the relative frequency bandwidth is $\Delta\nu/\nu_0 \approx 10^{-3}$. But for a 100 times shorter pulse ($\Delta t = 10$ fs), $\Delta\nu/\nu_0 \sim 0.1$. As $|\Delta\lambda/\lambda_0| = \Delta\nu/\nu_0$, the wavelength extension of this pulse is 62 nm, covering 15 % of the visible window of the electromagnetic spectrum. Taking into account the wings of the spectrum, a 10 fs pulse actually covers most of the visible window!
- Equality to 1/2 in 2.12 can only be reached with Gaussian time and spectral envelopes. The Gaussian pulse shape “consumes” a minimum amount of spectral components. When the equality is reached in (2.12), the pulse is called a Fourier-transform-limited pulse. The phase variation of such a pulse has a linear time dependence as described by (2.9); in other words, the instantaneous frequency is time-independent.
- For a given spectrum, one pulse envelope can be constructed that has the shortest possible duration.
- The shortest constructed pulse can only be transform-limited if its spectrum is symmetrical.
- If a transform-limited pulse is not Gaussian-shaped, then the equality in an expression similar to 2.12 applies, but for a constant quantity larger than 1/2 which depends on the shape of the pulse.

From the experimental point of view, half-maximum quantities are easier to measure; the Fourier inequality is then usually written as $\Delta\nu \Delta t = K$, where

$\Delta\nu$ is the frequency full width at half-maximum and Δt the half maximum duration. K is a number which depends on the shape of the pulse. Table 2.1 gives values of K for some symmetrical pulse shapes.

Shape	$\varepsilon(t)$	K
Gaussian function	$\exp[-(t/t_0)^2/2]$	0.441
Exponential function	$\exp[-(t/t_0)/2]$	0.140
Hyperbolic secant	$1/\cosh(t/t_0)$	0.315
Rectangle	—	0.892
Cardinal sine	$\sin^2(t/t_0)/(t/t_0)^2$	0.336
Lorentzian function	$[1 + (t/t_0)^2]^{-1}$	0.142

Table 2.1. Values of K for various pulse shapes, in the inequality $\Delta\nu \Delta t \geq K$, when $\Delta\nu$ and Δt are half-maximum quantities

Let us now consider a simple Gaussian light pulse

$$E_y = \text{Re} \left(E_0 e^{(-\Gamma t^2 + i\omega_0 t)} \right). \quad (2.13)$$

The instantaneous frequency is obtained by calculating the time derivative of the phase,

$$\omega(t) = \partial\Phi/\partial t = \omega_0. \quad (2.14)$$

In this situation the angular frequency is constant and equals the central angular frequency ω_0 . The light pulse is transform-limited; $\Delta\nu \Delta t = 0.441$. Let us now suppose that the phase of the pulse obeys a quadratic law in time,

$$E_y = \text{Re} \left(E_0 e^{[-\Gamma t^2 + i(\omega_0 t - \alpha t^2)]} \right), \quad \Gamma \in \Re, \quad (2.15)$$

then the instantaneous angular frequency varies linearly with time (Fig. 2.7):

$$\omega(t) = \partial\Phi/\partial t = \omega_0 + \alpha t, \quad \alpha > 0. \quad (2.16)$$

When a quadratic time dependence is added to the original phase term, the instantaneous frequency is more red in the leading part of the pulse and more blue in the trailing part (compare Fig. 2.4). The pulse is said to be “chirped.” This result describes the self-phase modulation process in the limit when $t \ll \Gamma$ (see (2.54) and (2.57)).

2.2.4 Propagation of a Light Pulse in a Transparent Medium

What happens to a short optical pulse propagating in a transparent medium? Because of its wide spectral width and because of group velocity dispersion in transparent media, it undergoes a phase distortion inducing an increase of its duration. This happens with any optical element and needs to be properly corrected for in the course of experiments.

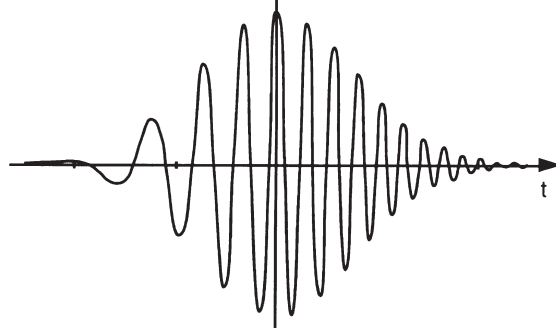


Fig. 2.7. Time evolution of the electric field in a Gaussian pulse having a quadratic time dependence of the phase

The frequency Fourier transform of a Gaussian pulse has already been given as

$$E_0(\omega) = \exp\left(\frac{-(\omega - \omega_0)^2}{4\Gamma}\right). \quad (2.17)$$

After the pulse has propagated a distance x , its spectrum is modified to

$$E(\omega, x) = E_0(\omega) \exp[-ik(\omega)x], \quad k(\omega) = n\omega/c, \quad (2.18)$$

where $k(\omega)$ is now a frequency-dependent propagation factor. In order to allow for a partial analytical calculation of the propagation effects, the propagation factor is rewritten using a Taylor expansion as a function of the angular frequency, assuming that $\Delta\omega \ll \omega_0$ (this condition is only weakly true for the shortest pulses). Applying the Taylor's expansion

$$k(\omega) = k(\omega_0) + k'(\omega - \omega_0) + \frac{1}{2}k''(\omega - \omega_0)^2 + \dots, \quad (2.19)$$

where

$$k' = \left(\frac{dk(\omega)}{d\omega}\right)_{\omega_0} \quad (2.20)$$

and

$$k'' = \left(\frac{d^2k(\omega)}{d\omega^2}\right)_{\omega_0}, \quad (2.21)$$

to 2.18, the pulse spectrum becomes

$$E(\omega, x) = \exp\left(-ik(\omega_0)x - ik'x(\omega - \omega_0) - \left(\frac{1}{4\Gamma} + \frac{i}{2}k''\right)(\omega - \omega_0)^2\right). \quad (2.22)$$

The time evolution of the electric field in the pulse is then derived from the calculation of the inverse Fourier transform of 2.22,

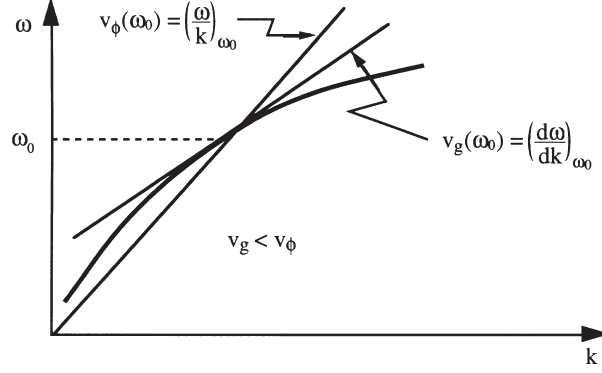


Fig. 2.8. Schematic relationship between the phase and group velocities in an ordinary transparent medium. Note that this relationship does not depend on the sign of the curvature of the dispersion curve $\omega(k)$

$$\varepsilon(t, x) = \frac{1}{2\pi} \int_{-\infty}^{+\infty} E(\omega, x) e^{i\omega t} d\omega, \quad (2.23)$$

so that

$$\varepsilon(t, x) = \sqrt{\frac{\Gamma(x)}{\pi}} \exp \left[i\omega_0 \left(t - \frac{x}{v_\phi(\omega_0)} \right) \right] \times \exp \left[-\Gamma(x) \left(t - \frac{x}{v_g(\omega_0)} \right)^2 \right], \quad (2.24)$$

where

$$v_\phi(\omega_0) = \left(\frac{\omega}{k} \right)_{\omega_0}, \quad v_g(\omega_0) = \left(\frac{d\omega}{dk} \right)_{\omega_0}, \quad \frac{1}{\Gamma(x)} = \frac{1}{\Gamma} + 2ik''x. \quad (2.25)$$

In the first exponential term of 2.24, it can be observed that the phase of the central frequency ω_0 is delayed by an amount x/v_ϕ after propagation over a distance x . Because the phase is not a measurable quantity, this effect has no observable consequence. The phase velocity $v_\phi(\omega)$ measures the propagation speed of the plane-wave components of the pulse in the medium. These plane waves do not carry any information, because of their infinite duration.

The second term in 2.24 shows that, after propagation over a distance x , the pulse keeps a Gaussian envelope. This envelope is delayed by an amount x/v_g , v_g being the group velocity. Figure 2.8 shows schematically the relationship between the phase and the group velocities.

The phase velocity $v_\phi(\omega_0) = (\omega_0/k)$ is the slope of a straight line starting at the origin and crossing the dispersion curve $\omega(k)$ where the angular frequency equals ω_0 . The group velocity $v_g(\omega_0) = (d\omega/dk)_{\omega_0}$ is the slope of the line tangential to the dispersion curve at the same point. In ordinary matter, $v_g < v_\phi$.

From the expression for the propagation factor $k = 2\pi/\lambda$ and the expression for the wavelength in a medium $\lambda = 2\pi c/\omega n(\omega)$, $n(\omega)$ being the index of

refraction, one gets

$$v_\phi = \frac{c}{n(\omega)}, \quad (2.26)$$

$$v_g = \frac{d\omega}{dk} = \frac{1}{(dk/d\omega)}, \quad \frac{dk}{d\omega} = \frac{1}{c} \left(n(\omega) + \omega \frac{dn(\omega)}{d\omega} \right), \quad (2.27)$$

$$v_g \approx v_\phi \left(1 - \frac{\omega}{n(\omega)} \frac{dn(\omega)}{d\omega} \right). \quad (2.28)$$

The second term in 2.24 also shows that the pulse envelope is distorted during its propagation because its form factor $\Gamma(x)$, defined as

$$\frac{1}{\Gamma(x)} = \frac{1}{\Gamma} + 2ik''x, \quad (2.29)$$

depends on the angular frequency ω through $k''(\omega)$,

$$k'' = \left(\frac{d^2k}{d\omega^2} \right)_{\omega_0} = \frac{d}{d\omega} \left(\frac{1}{v_g(\omega)} \right)_{\omega_0}. \quad (2.30)$$

This term is called the “group velocity dispersion”.

Rewriting $\Gamma(x)$ as

$$\Gamma(x) = \frac{\Gamma}{1 + \xi^2 x^2} - i \frac{\Gamma \xi x}{1 + \xi^2 x^2}, \quad \xi = 2\Gamma k'' \quad (2.31)$$

and substituting 2.31 into the second term of the right-hand side of 2.24 yields the following expression:

$$\exp \left[-\frac{\Gamma}{1 + \xi^2 x^2} \left(t - \frac{x}{v_g} \right)^2 + i \frac{\Gamma \xi x}{1 + \xi^2 x^2} \left(t - \frac{x}{v_g} \right)^2 \right]. \quad (2.32)$$

The real part of 2.32 is still a delayed Gaussian function. Its form factor

$$\frac{\Gamma}{1 + \xi^2 x^2} \quad (2.33)$$

is always smaller than the original one Γ , which means that the pulse undergoes a duration broadening. Figure 2.9 shows a sketch of the pulse envelope broadening during its propagation through a transparent medium.

The phase, i.e. imaginary part in 2.32, contains a quadratic time term and we have already seen that this creates a linear frequency chirp in the pulse (Sect. 2.2.3).

In summary, the propagation of a short optical pulse through a transparent medium results in a delay of the pulse, a duration broadening and a frequency chirp.

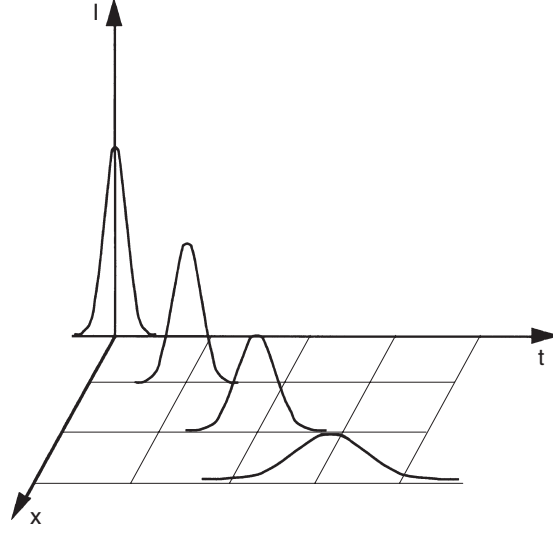


Fig. 2.9. Numerical calculation of the intensity envelope of a pulse propagating along x , in a lossless, transparent medium. The pulse broadens with time but, from energy conservation, its time-integrated intensity remains constant

2.2.4.1 Dispersion Parameter of a Transparent Medium. The dispersion of an index of refraction is usually tabulated as a function of the wavelength of light in vacuum. We therefore need to recalculate the dispersion as a function of the wavelength. From 2.30 we obtain

$$k'' = -\frac{\lambda^2}{2\pi c} D, \quad D = \frac{1}{L} \frac{dt_g}{d\lambda}, \quad (2.34)$$

with t_g being the group delay induced by propagation over length L . D is called the dispersion parameter. The group delay t_g is calculated using 2.28 for the group velocity and the simple definition $t_g = L/v_g$, which leads to

$$k'' = \frac{\lambda^3}{2\pi c^2} \frac{d^2 n}{d\lambda^2}. \quad (2.35)$$

The sign of k'' depends on the curvature of the dispersion of the index $d^2 n/d\lambda^2$.

A one-resonance Drude model is the simplest way to describe the electronic properties of matter. In this very simple model the variation of the index of refraction in the vicinity of the resonance looks as shown in Fig. 2.10.

For wavelengths larger than the resonance wavelength the curvature of the index dispersion curve is positive (upward concavity) and the group velocity dispersion is positive ($k'' > 0$). This situation is the most usual one, encountered in ordinary optical glasses in the visible range. The index of refraction diminishes as the wavelength increases, which in turn implies an increase of

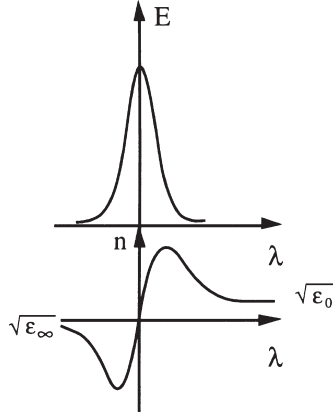


Fig. 2.10. (*Top*) sketch of an electronic resonance, from which the index of refraction (*bottom*) can be calculated

the group velocity: in a light pulse propagating through a transparent medium, the instantaneous frequency varies from its lowest value in the leading edge to its highest value in the trailing edge. Notice from 2.34 that a positive group velocity dispersion corresponds to a negative dispersion parameter D .

For wavelengths below the electronic resonance the situation is reversed and the group velocity dispersion is negative. This situation can be found in silica optical fibers, where a single resonance takes place, due to OH vibrations. For wavelengths around $1.55\ \mu\text{m}$, the group velocity is negative, allowing the propagation of optical solitons.

2.2.4.2 Time Compression with a Pair of Gratings. In order to correct for group-velocity-dispersion distortions, several optical devices have been designed that have an overall negative group velocity dispersion. As an example we consider a pair of transmission gratings R_1 and R_2 . These gratings have a groove spacing d and their separation is l (Fig. 2.11).

A light ray, with wavelength λ , impinges on grating R_1 with an angle of incidence γ and is scattered with an angle θ . The gratings are set in such a way that their wavelength dispersions are reversed, which implies that the exiting ray at point B is parallel to the incident ray. P_1 and P_2 are wave planes at the entrance A and exit B of the system. P_2 crosses the emerging ray at point C. Between points A and B the light travels a distance $b = l / \cos \theta$. The diffraction due to a grating can be written as

$$d(\sin \gamma + \sin \theta) = \lambda. \quad (2.36)$$

In order to calculate the dispersion from 2.34, the group delay experienced by the light must first be evaluated. In this specific case, where propagation takes place only in air, the group delay is simply equal to the travel time of

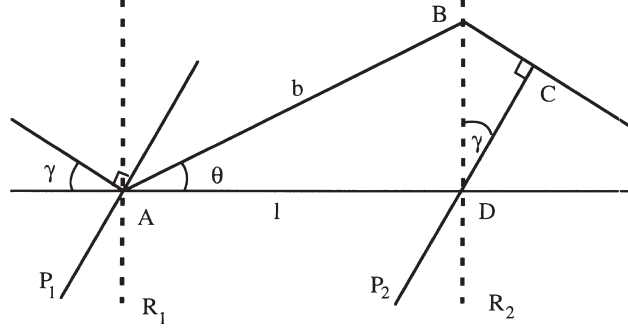


Fig. 2.11. Optical path through a pair of transmission gratings

light along ABC,

$$t = L/c = (AB + BC)/c, \quad BC = DB \sin \gamma = b \sin \theta \sin \gamma, \quad (2.37)$$

$$t = \frac{b}{c}(1 + \sin \theta \sin \gamma), \quad (2.38)$$

and the dispersion parameter is expressed as

$$D = \frac{1}{b} \frac{dt}{d\lambda}, \quad (2.39)$$

which from 2.36, applying a small-angle approximation, yields

$$D = \frac{\lambda}{cd^2} \left[1 - \left(\frac{\lambda}{d} - \sin \gamma \right)^2 \right]^{-1}, \quad (2.40)$$

$$k'' = -\frac{\lambda^3}{2\pi c^2 d^2} \left[1 - \left(\frac{\lambda}{d} - \sin \gamma \right)^2 \right]^{-1}. \quad (2.41)$$

This expression demonstrates the possibility of selecting a set of parameters in such a way as to design a pair of gratings producing a positive or a negative group velocity dispersion. Therefore optical devices can be built that compensate a positive group velocity dispersion suffered by optical pulses travelling through a transparent material. Optical compressors have been a key to the development of various fields in which short optical pulses have been used as a primary tool. Figure 2.12 shows a typical arrangement for a reflective pulse compressor.

2.3 Nonlinear Optics

2.3.1 Second-Order Susceptibility

The second-order susceptibility $\chi^{(2)}$ governs several nonlinear optical effects, some of which will be considered in this section. Second-harmonic generation

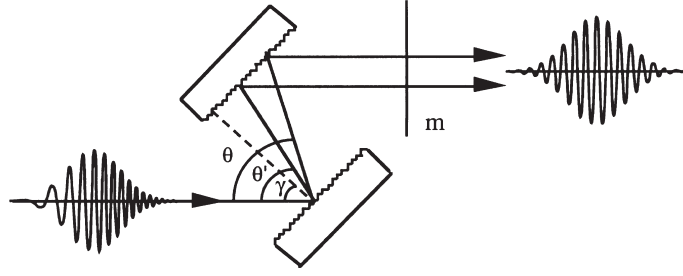


Fig. 2.12. Grating optical compressor. Two gratings are set in a subtractive diffraction geometry. Red components of a light pulse have a longer optical path than blue ones. The various components of a positively dispersed pulse can therefore be reset in phase

will be explored in some detail, while other effects will only be mentioned because of their importance in the physics of pulsed lasers.

2.3.1.1 Second-Harmonic Generation. Second-harmonic generation was the first nonlinear optical effect to be observed after lasers became available.

In this process, two photons having the same angular frequency ω , when propagating through a suitable material, can mix together, giving rise to a single photon with twice the original frequency. In the framework of classical physics, light propagation is described in terms of coherent emission by harmonic electronic dipoles, which have been set to oscillate by the light itself. This picture can be extended to the nonlinear regime by assuming that at high excitation intensities (meaning large oscillation amplitude of the electronic oscillators), the oscillations become strongly anharmonic. Under this assumption, the emitting dipoles can radiate energy at frequencies which are integer multiples of the original frequency.

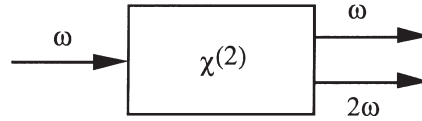


Fig. 2.13. When a noncentrosymmetric crystal is illuminated with photons with angular frequency ω some pairs of these photons disappear, replaced by single photons with angular frequency 2ω . This effect is called second-harmonic generation

The polarization of a material can be written as

$$P_i(2\omega) = \sum_{j,k} \chi_{ijk}^{(2)} E_j(\omega) E_k(\omega). \quad (2.42)$$

In a dipole approximation of the electron–photon interaction, the second-order susceptibility $\chi^{(2)}$ is a third-order tensor, with components corresponding to

the various possible orientations of the crystal axis and of light polarization. In the specific case in which the structure of the medium has an inversion centre the tensor is identical to zero: no second harmonic can be generated (the central symmetry of a material is relaxed on its surface and mixing of photons is possible there with a weak yield). In the ideal case of a plane wave the intensity of the generated second harmonic is as follows:

$$I(2\omega) = \frac{2^7 \pi^3 \omega^2 \chi_{\text{eff}}^2 l^2}{n^3 c^3} I^2(\omega) \left(\frac{\sin(\Delta k l / 2)}{\Delta k l / 2} \right)^2. \quad (2.43)$$

The dependence on both the length of the material l and the incident intensity $I(\omega)$ is quadratic; n is the index of refraction and c the velocity of light. The intensity of the doubled frequency is proportional to the square of an effective susceptibility $\chi_{\text{eff}}^{(2)}$, which depends on the material and reflects the mean doubling properties of this material in a given working direction. For the doubling yield to be maximum, the dephasing quantity $\Delta k = k_2 - 2k_1$ must be zero. This dephasing term accounts for the propagation effects during the doubling process. At any one point along the propagation axis the electronic oscillators radiate at angular frequency ω and 2ω in the same direction k . After propagation over a distance l in the medium the fundamental frequency generates the second-harmonic frequency with a time delay $k_1 l$, while the previously generated second harmonic reaches the same point with a time delay $k_2 l$. If the distance l is such that the dephasing quantity $\Delta k l = (k_2 - 2k_1)l$ is zero, then the two contributions add constructively; otherwise they interfere destructively.

The coherence length of a doubling crystal is defined as the characteristic distance along which the second-harmonic waves remain in phase, and it can be calculated using (2.43). To achieve efficient frequency-doubling devices it is now clearly apparent that dephasing must be overcome. The most common way to do this is to use birefringent crystals for which the ordinary and extraordinary index surfaces for the fundamental and doubled frequencies cross one another (Fig. 2.14).

In the propagation directions defined by these intersections, the indices of refraction at the fundamental and doubled frequencies are equal and the phase mismatch quantity $\Delta k = 0$. When this condition is fulfilled, the sinc function in (2.43) is equal to unity and the coherence length is infinite. Calculation of the phase-matching angle θ_c between the propagation direction, taken orthogonal to the surface of the crystal, and the c axis of the crystal can be made using

$$\left(\frac{1}{n_e^{2\omega}(\theta)} \right)^2 = \frac{\sin^2 \theta}{(n_e^{2\omega})^2} + \frac{\cos^2 \theta}{(n_o^{2\omega})^2} = \left(\frac{1}{n_o^\omega(\theta)} \right)^2. \quad (2.44)$$

Various situations can be encountered depending on the birefringent crystal: in positive crystals, like quartz, $n_e > n_o$, while in negative crystals, like calcite, $n_e < n_o$. For type I phase-matching crystals the two mixing photons have the

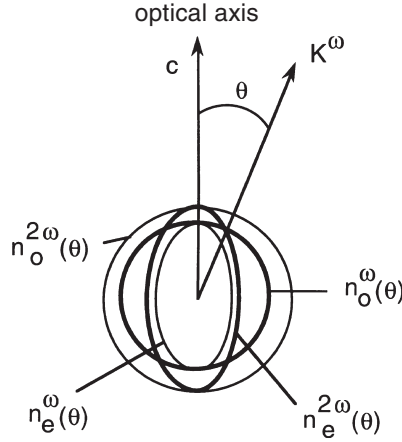


Fig. 2.14. *Thin lines:* intersection of the plane containing the c axis of a birefringent crystal with its ordinary index surfaces. *Thick lines:* intersection with the extraordinary surfaces

same polarization direction, while in type II crystals they are orthogonally polarized.

Nowadays excellent doubling efficiencies are reached, close to 100 % in some cases.

Because of their wide spectral width, doubling of ultrashort light pulses needs special care. The doubling bandwidth of the crystal must accommodate the full spectral width of the pulse. For a negative uniaxial crystal, such as KDP, the wavelength bandwidth can be written as

$$d\lambda_1 = \frac{\pm 1.39\lambda_1}{2\pi l} \left(\frac{\partial n_o^\omega}{\partial \lambda_1} - \frac{1}{2} \frac{\partial n_e^{2\omega}}{\partial \lambda_2} \right), \quad (2.45)$$

where λ_1 and λ_2 are the wavelengths of the light at the fundamental and doubled frequencies. Examination of 2.45 shows that to enlarge the doubling bandwidth of a crystal one has to decrease its thickness l , which of course is detrimental to the conversion yield, which is proportional to the square of that thickness (see (2.43)). The first ultrashort pulses ever produced, 6 fs at 620 nm, have been characterized using a second-harmonic autocorrelation technique based on a 30 μm thick KDP crystal. Increasing the thickness of the crystal would have reduced its bandwidth, leading to an overestimation of the duration of the pulses.

Real life is always more complex: even if a perfect phase-matching is achieved, group velocity dispersion remains different for the fundamental and the doubled frequencies, inducing time broadening of the pulses.

2.3.1.2 Parametric Interactions. The second-order susceptibility is responsible for a large variety of other effects involving three photons and gener-

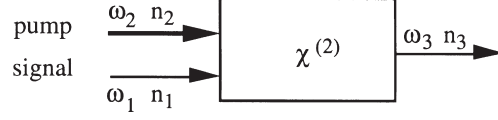


Fig. 2.15. Second-order susceptibility is responsible for various parametric effects, in which one photon is split into two other ones or two photons are mixed

ating new frequencies. These effects are called parametric effects, as a reference to forced oscillators and related techniques, which were previously developed in the field of radio-frequency electronics.

A classification of these parametric effects can be based on energy and momentum conservation for the three photons involved in the process. A nonlinear crystal with second-order susceptibility $\chi^{(2)}$ is illuminated with an intense pump pulse containing n_2 photons at angular frequency ω_2 and a weak signal pulse containing n_1 photons at angular frequency ω_1 ; n_3 photons are emitted with angular frequency ω_3 . Such a classification is given in Table 2.2.

Photon number $\omega_1 > \omega_2$ variation		$\omega_1 < \omega_2$	Photon number variation
$n_1 - 1$	Frequency difference	Frequency sum	$n_1 - 1$
$n_2 + 1$	$\omega_3 = \omega_1 - \omega_2$	$\omega_3 = \omega_2 + \omega_1$	$n_2 - 1$
$n_3 + 1$	$k_1 = k_2 + k_3$	$k_3 = k_1 + k_2$	$n_3 + 1$
$n_1 - 1$	Frequency sum	Parametric amplification	$n_1 + 1$
$n_2 - 1$	$\omega_3 = \omega_1 + \omega_2$	$\omega_3 = \omega_2 - \omega_1$	$n_2 - 1$
$n_3 + 1$	$k_3 = k_1 + k_2$	$k_2 = k_1 + k_3$	$n_3 + 1$

Table 2.2. Optical parametric interactions ordered according to energy and momentum conservation

$\omega_1 > \omega_2$. The pump frequency is smaller than the signal frequency. There are two cases to consider.

- *Case 1.* One photon with angular frequency ω_1 is annihilated (photon number becomes $n_1 - 1$) while two photons with angular frequencies ω_2 ($n_2 + 1$) and ω_3 ($n_3 + 1$) are created. Energy conservation implies the equality $\omega_3 = \omega_1 - \omega_2$. Every parametric interaction is a coherent effect which must respect a phase-matching condition between the various waves propagating in the crystal; this is implied by momentum conservation, $k_1 = k_2 + k_3$. In this case photons are emitted with a frequency which is equal to the frequency difference between the two incident photons. The signal (ω_1) intensity decreases (n_1 decreases), while the intensity of the pump (ω_2) and the frequency difference (ω_3) increase.

- *Case 2.* One photon with angular frequency ω_1 is destroyed ($n_1 - 1$) along with a pump photon (ω_2) ($n_2 - 1$), while one photon is created ($n_3 + 1$) with angular frequency ω_3 . Energy conservation implies $\omega_3 = \omega_1 + \omega_2$ while momentum conservation implies $k_3 = k_1 + k_2$. This parametric effect is called “up-conversion”. The pump and signal intensities decrease, favoring the resulting emission, contrary to Case 1, in which the pump intensity increases.

As in the case of second-harmonic generation, these processes can only take place in crystals having a large $\chi^{(2)}$, and where there are propagation directions allowing index matching and momentum conservation. When these prerequisites are fulfilled, waves produced in phase can add constructively, giving rise to significant light intensities. Selection of one effect or the other is realized by adjusting the angles of incidence of the incident light beams with respect to the crystal axes.

In a semiclassical model in which only the electronic system is quantized, these effects are described, in the transparency regime, via virtual electronic transitions. Therefore, as they are not related to any specific electronic resonance, tunability can be achieved by adjusting the incidence angles of the beam, on the crystal. However, the tunability bandwidth is limited by the phase-matching condition. On any timescale down to a few femtoseconds these effects can be considered as instantaneous.

$\omega_1 < \omega_2$. The pump frequency is greater than the signal frequency. Again, there are two cases.

- *Case 1* corresponds again to up-conversion with a reversal of the roles played by the pump and the signal, compared to the previous Case 2.
- *Case 2.* One photon with angular frequency ω_2 is destroyed ($n_2 - 1$) while two photons are created, one with the signal frequency ω_1 ($n_1 + 1$) and one with the new frequency ω_3 ($n_3 + 1$), in such a way as to ensure $\omega_2 = \omega_1 + \omega_3$ and $k_2 = k_1 + k_3$. This is called “optical parametric amplification” (OPA) because the weak signal is amplified, in contrast to the strong pump intensity.

Other combinations could be added to the table which would not respect the realistic condition that a frequency must be positive. For example, one cannot expect a process to start with the destruction of a photon with angular frequency ω_3 .

These effects are not totally independent. Let us consider, for example, the parametric frequency difference effect. For long enough propagation paths in matter, the implicit assumption that there is no depletion of the beams is not necessarily valid; the intensity of the signal can drop to 0 ($n_1 = 0$). The process then stops but the situation is such that up-conversion may start, one photon with angular frequency ω_3 mixing with one photon with angular frequency ω_2 .

2.3.1.3 Spontaneous Parametric Fluorescence. Spontaneous parametric fluorescence is a special case of the parametric amplification process, in which the signal with angular frequency $\omega_1 < \omega_2$ is turned off. A $\chi^{(2)}$ nonlinear crystal spontaneously emits radiation with angular frequency ω_1 and ω_3 when irradiated with a strong pump beam made up of photons with angular frequency ω_2 such that $\omega_3 = \omega_2 - \omega_1$ and $k_1 + k_3 = k_2$. Although only a quantum-mechanical treatment can rigorously account for this effect, a rather good classical picture is to consider the effect as being started by the ambient noise, replacing the ω_1 signal photons. For a given orientation of the nonlinear crystal, numerous photons simultaneously satisfy the energy and momentum conservation conditions and therefore the spectral bandwidth of the parametric emission is large. This is being widely studied for the amplification of stretched ultrashort light pulses.

2.3.1.4 Applications of Parametric Effects. Second-harmonic generation is by far the most commonly used optical nonlinear effect in the field of lasers. Argon ion lasers are poor converters of electrical energy to light; a 10^{-3} conversion yield is a good figure. Solid-state lasers, on the contrary, are more efficient converters, for which a yield ten times larger is readily achievable. Nd:YAG, Nd:YLF, Nd:glass, etc. lasers emit light around $1.06 \mu\text{m}$ and it is therefore of useful policy to double this frequency, since a 30 % doubling yield is easy to realize. This is clearly illustrated by the introduction onto the market of doubled frequency diode-pumped solid-state lasers, generating more than 5 W of CW green light, needing only a regular electrical socket as an energy source. Doubling is also commonly used for ultrashort pulse metrology.

Up-conversion, also used to increase the frequency of laser pulses, is useful as well for time resolution of photoluminescence. The spontaneous emission of a material can be mixed in a $\chi^{(2)}$ nonlinear crystal with a short reference, pulse allowing a spectro-temporal study of the emission. Detectors in the infrared spectrum are less sensitive than their equivalents in the visible range, so it can be of great interest to up-convert a weak signal to the visible range, using a strong pump. More applications are described in some detail in the following chapters.

OPA. Optical parametric amplification has already been described above and we have learned that the angular frequencies ω_1 and ω_3 are amplified via an intensity decrease of the pump. This amplification process should not be confused with the amplification by stimulated emission in a medium which has an inverted electronic population. Because of the instantaneous character of the process there is no time delay between excitation and emission.

The Manley–Rowe equation

$$-\Delta\left(\frac{I_2}{\omega_2}\right) = \Delta\left(\frac{I_1}{\omega_1}\right) \Delta\left(\frac{I_3}{\omega_3}\right) \quad (2.46)$$

relates the intensity variations of the various beams. Using a LiNbO_3 crystal having a susceptibility $\chi_{\text{eff}}^{(2)} = 0.5 \times 10^{-22} \text{ MKS}$, pumped in the vicinity of

$\lambda_2 = 1\text{ }\mu\text{m}$ with an intensity $I_2 = 10^6\text{ W/cm}^2$, a gain of only 0.667 cm^{-1} is reached for the emitted wavelengths $\lambda_3 = 3\text{ }\mu\text{m}$ and $\lambda_1 = 0.5\text{ }\mu\text{m}$. Parametric gains are always low and are of best use in laser cavities.

OPO. An optical parametric oscillator is a laser in which the optical gain is produced in a parametric crystal rather than by an electronic inverted population. The analysis of this application is beyond the scope of this short introduction and is usually described in quantum-electronics textbooks. We will merely point out that one can set up laser cavities oscillating at both amplified frequencies or only one, depending on needs.

These techniques are developing rapidly and are worth the work they imply, because of the nonresonant character of the parametric amplification process, which allows the tuning of the emitted light by adjustment of the phase-matching angles. In practice this means that tunability is achieved by orienting a nonlinear crystal with respect to the axis of an optical resonator.

The parametric techniques have already reached a point of development which makes them commercially available. Several companies are presently competing in niche markets.

2.3.2 Third-Order Susceptibility

Four photons are involved in the nonlinear optical effects due to the third-order susceptibility term of the expansion of the polarization of a material. In contrast with second-order effects, the various third-order effects do not vanish in centrosymmetric materials and they can be observed in liquids or amorphous materials, such as fused silica for instance. For all the possible effects, energy and momentum are conserved quantities and phase-matching conditions must be fulfilled.

One of the possible effects is the mixing of two photons of a laser beam in a $\chi^{(3)}$ nonlinear medium, generating two frequency-shifted photons such that $2\omega_L = \omega_1 + \omega_2$, with $\omega_1 > \omega_L$ and $\omega_2 < \omega_L$. When two laser beams are present a more general interaction occurs, such as, for instance, the mixing of three photons into one high-frequency photon. A single photon can also split into three lower-frequency photons. However, the efficiency of these effects is always poor. Degenerate and nondegenerate four-wave mixing have no popular application in the field of lasers; rather, they are used for the measurement of energy and phase relaxation dynamics in matter.

Stimulated fluorescence, amplification and Raman and Brillouin scattering, as well as two-photon absorption, belong to this class of $\chi^{(3)}$ effects. Obviously the number of observable effects is a rapidly growing function of the susceptibility order, and we will now focus only on the variations of the index of refraction induced by a strong pulse in a transparent isotropic medium.

2.3.2.1 Nonlinear Index of Refraction. When an intense electromagnetic wave passes into an isotropic medium its dielectric response is changed:

$$\varepsilon_t = \varepsilon + \varepsilon_2 \langle \mathbf{E} \cdot \mathbf{E} \rangle. \quad (2.47)$$

Where $\langle \mathbf{E} \cdot \mathbf{E} \rangle$ is the time average of the squared electric field. Therefore $\langle \mathbf{E} \cdot \mathbf{E} \rangle = \frac{1}{2} |\mathbf{E}|^2$. It can be demonstrated that such a dielectric function occurs when the polarization is written as

$$\mathbf{P} = \varepsilon_0 \chi^{(1)} + \varepsilon_0 \chi^{(3)} \langle \mathbf{E} \cdot \mathbf{E} \rangle \mathbf{E}; \quad (2.48)$$

therefore $\varepsilon = 1 + \chi^{(1)}$ and $\varepsilon_2 = 1 + \chi^{(3)}$. The $\chi^{(2)}$ term is zero because of the choice of a centrosymmetric medium.

As the index of refraction is given by the square root of the dielectric function, one easily finds that

$$n = \sqrt{\varepsilon_t} = \sqrt{\varepsilon + \varepsilon_2 \langle \mathbf{E} \cdot \mathbf{E} \rangle} \approx n_0 + n_2 \langle \mathbf{E} \cdot \mathbf{E} \rangle \quad (2.49)$$

and one eventually gets

$$n = n_0 + \frac{1}{2} n_2 I, \quad (2.50)$$

where $I = |\mathbf{E}|^2$ is the intensity of the light.

Numerous physical effects can yield a nonlinear polarization of the form $\varepsilon_0 \chi^{(3)} \langle \mathbf{E} \cdot \mathbf{E} \rangle \mathbf{E}$ and therefore an intensity-dependent index of refraction.

When an applied electric field is strong enough the electronic cloud of an atom or a molecule is strongly distorted. This happens when the mean electrostatic energy of the field $\frac{1}{2} \varepsilon_0 \varepsilon \langle \mathbf{E} \cdot \mathbf{E} \rangle EV$ (V being the interaction volume) becomes comparable to the energy of the electronic states (a few eV). Also the rotational Kerr effect can take place in liquids with anisotropic dissolved molecules whose polarisability is different along their large and small axes. A linearly polarized electric field favors the alignment of one of the axis of the molecules along its direction. This effect is generally stronger than the electric-field effect; it is also slower because it involves the full mass of the molecules instead of only the mass of the electrons.

From 2.50 we know that in the $\chi^{(3)}$ limit the change of index of refraction in a transparent medium is simply proportional to the intensity of the applied electric field. Closer examination also indicates that properties of the intensity distribution must be mapped onto the index change. Generally speaking, the light emitted by a pulsed laser is distributed in both space and time, $I = I(\mathbf{r}, t)$.

The analysis of the nonlinear propagation of a light pulse is a complex problem which needs numerical approaches; we will only consider situations which can be studied analytically.

2.3.2.2 Kerr Lens Effect. We will start with the spatial dependence of the light intensity and for the sake of simplicity we will study the propagation of a Gaussian laser beam in a $\chi^{(3)}$ material. This beam is described by a Gaussian function of its radius with shape parameter g . In this case the index distribution can be written as:

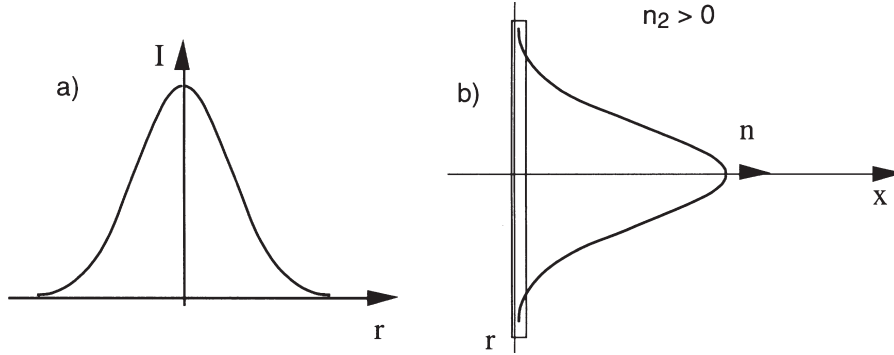


Fig. 2.16. (a) Intensity distribution of a Gaussian beam along one of its diameters. (b) Assuming the propagation of this intensity distribution along the x direction in a thin slab of $\chi^{(3)}$ material, the variation of the index of refraction follows the intensity distribution along the diameter. Depending on the sign of the nonlinear index of refraction, the index of refraction increases ($n_2 > 0$) or decreases ($n_2 < 0$) when going toward the center of the laser beam

$$n(r) = n_0 + \frac{1}{2}n_2I(r), \quad \text{with } I(r) = e^{-gr^2}. \quad (2.51)$$

Figure 2.16a shows the intensity distribution along a diameter of a Gaussian beam. If this beam is propagating through a thin slab of $\chi^{(3)}$ transparent material (Fig. 2.16b), then the index change follows the intensity along that same diameter. For a positive n_2 the index of refraction is larger at the center of the slab than at the side. In the framework of geometrical optics, the quantity relevant to the propagation of a light ray is the optical path, i.e. the product of the index of refraction and the propagation distance e , $P(r) = n(r)e$. To visualize the Kerr lens effect we replace the constant thickness e by a variable one such that its product with a constant index of refraction leads to the same optical path:

$$P(r) = n(r)e = e(r)n_0. \quad (2.52)$$

Then

$$e(r) = \frac{en(r)}{n_0} \quad (2.53)$$

and one gets a Gaussian lens, which focuses the optical beam. During the propagation of a pulse through a thick material (Fig. 2.17) this process is enhanced along the path because focusing of the beam increases the focal power of the dynamical lens. This increase of the focusing stops when the diameter of the beam is small enough so that the linear diffraction is large enough to balance the Kerr effect. This effect, named self-focusing, is of prime importance in the understanding of self-mode-locking, or Kerr lens mode-locking (KLM) which occurs in titanium-doped sapphire lasers.

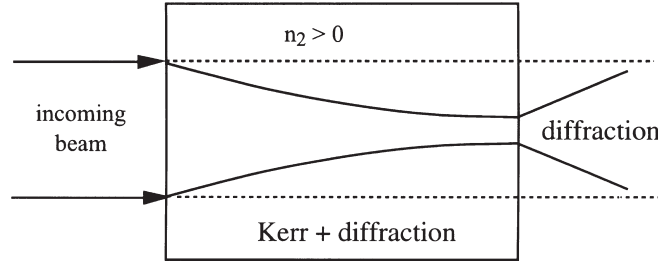


Fig. 2.17. Self-focusing of a laser beam crossing a medium with positive n_2

2.3.2.3 Self-Phase-Modulation. Similarly, the nonlinear index of a material depends on the time dependence of a light pulse intensity envelope, which can be expressed as

$$n = n_0 + \frac{1}{2}n_2 I(t), \quad \text{with } I(t) = e^{-\Gamma t^2}. \quad (2.54)$$

What is the influence of this time-varying index on the frequency of the light? To simplify the analysis we only consider a plane wave propagating in a non-linear medium:

$$E(t, x) = E_0 e^{i(\omega_0 t - kx)}, \quad k = \frac{\omega_0}{c} n(t). \quad (2.55)$$

The instantaneous frequency, being the time derivative of the phase, can be written as

$$\omega(t) = \frac{\partial}{\partial t} \Phi(t) = \omega_0 - \frac{\omega_0}{c} \frac{\partial n(t)}{\partial t} x \quad (2.56)$$

and the frequency variation as

$$\delta\omega(t) = \omega(t) - \omega_0 = -\frac{\omega_0 n_2}{2c} x \frac{\partial I(t)}{\partial t} \quad (2.57)$$

(Fig. 2.18).

As a very general consequence of the Fourier duality between time and frequency, any time a periodic amplitude or phase modulation is applied to a periodic signal new frequency components are created in its frequency spectrum. In the self-phase-modulation process, with n_2 positive, new low frequencies are created in the leading edge of the pulse envelope and new high frequencies are created in the trailing edge. These new frequencies are not synchronized, but are still created inside the original pulse envelope. Self-phase-modulation is not a dispersive effect in itself, but a pulse does not remain transform-limited when it crosses a transparent material. The transparent material in which the pulse propagates is dispersive, however, and therefore the frequencies are further chirped along the propagation.

Self-phase-modulation, because it opens the way to a spectral broadening of a light pulse, has been (and still is) the very basis of the optical compression

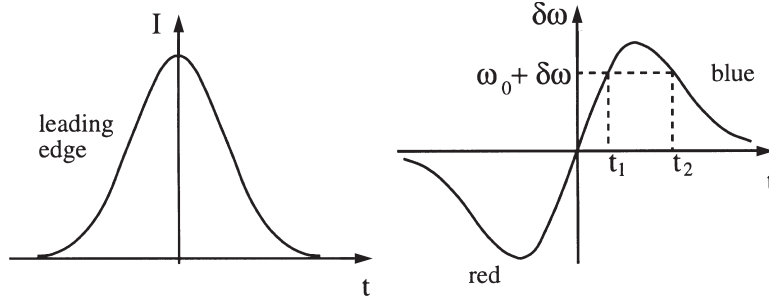


Fig. 2.18. *Left*, intensity dynamics of a Gaussian light pulse; the earlier times, i.e. the leading edge of the pulse, lie on the left side of the graph. *Right*, time variation of the central pulsation, which is proportional to the negative of the pulse envelope derivative when the nonlinear index of refraction is positive

technique used for producing ultrashort light pulses less than 10 fs in duration in the visible spectral range. When propagating light in a monomode silica fiber, only light with momentum along the fiber axis can be coupled; for that reason intense light pulses cannot undergo self-focusing, which would correspond to forbidden light momentum directions, and as a consequence self-phase-modulation is favored. Self-focusing down to the diffraction limit in sapphire leads to the generation of the large white light continua used as seeds in commercially available OPA.

Induced index variations can also be observed in degenerate or nondegenerate pump-and-probe experiments. A strong pump pulse can induce an index change in a medium, which can be experienced by a weak probe pulse. In the time domain the dynamical index change created by the pump shifts the central frequency of the probe. A record of the frequency shift versus time delay maps the derivative of the pump envelope. When n_2 is positive the probe frequency is red-shifted when it leads the pump pulse and blue-shifted when it trails the pump. This is the physical basis of the famous FROG technique used to simultaneously characterize phase and amplitude of short optical pulses (see Chap. 7). In the space domain the probe beam undergoes focusing, or defocusing as well as deflection, depending on the relative geometry of the pump and the probe beams.

Fourier transformation allows us to calculate the spectrum which results from the self-phase-modulation process. Figure 2.19 shows the spectrum of a self-phase-modulated pulse when the total nonlinearly induced phase shift is equal to 2π .

The spectral signature of self-phase-modulation is a “channeled” spectrum: as can be noticed from 2.57 and seen in Fig. 2.18, pairs of identical frequencies are created at two different time delays, t_1 and t_2 , inside the pulse envelope. For values ω of the angular frequency such that the time delay $t_2 - t_1 = n\pi/\omega$, n an odd integer, there is a destructive interference between the two

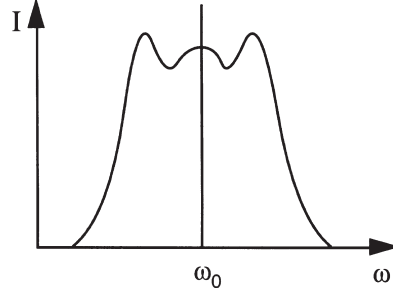


Fig. 2.19. Frequency spectrum of an originally Gaussian pulse which has suffered an induced phase shift equal to 2π

generated waves and a subsequent dip in the spectrum. At a time for which $t_2 - t_1 = n2\pi/\omega$ (n is an integer) the interference is constructive and the spectrum passes through a maximum. A simple examination of the spectrum therefore allows one to determine the maximum phase change and to estimate the absolute value of the nonlinear index of refraction.

Two other $\chi^{(3)}$ nonlinear effects are of great importance in the understanding of laser physics: gain saturation and absorption saturation. Gain saturation has already been examined in Chap. 1, so we will now only consider absorption saturation.

2.3.2.4 Saturable Absorbers. A saturable absorber is a material in which the transmittance increases with increasing light illumination. To describe the process we will consider simple qualitative arguments based on a two-level electronic model, for which saturable absorption is symmetrical to gain saturation. In this simple framework, a hyperbolic dependence of the absorption coefficient on the intensity is again a satisfactory approximation:

$$\alpha(I) = \alpha_0 \left(1 + \frac{I}{I_{\text{sat}}} \right)^{-1}, \quad (2.58)$$

where α_0 is the low-intensity (linear) absorption coefficient and I_{sat} is the saturation intensity, a phenomenological parameter.

For increasing intensities the absorption coefficient decreases, which translates for the transmitted intensity as

$$T(I_i) = \frac{I_t}{I_i} = \exp \left[\frac{-\alpha_0 L}{1 + I_i/I_{\text{sat}}} \right]. \quad (2.59)$$

Equation 2.59 is obtained by replacing the constant low-intensity absorption coefficient in the Beer–Lambert law $I_t = I_0 \exp(-\alpha_0 L)$ by expression 2.58. I_i is the intensity incident on the absorbing medium of length L , and I_t is the transmitted intensity. Figure 2.21 shows a numerical simulation of the transmission behavior as a function of the incoming light intensity.

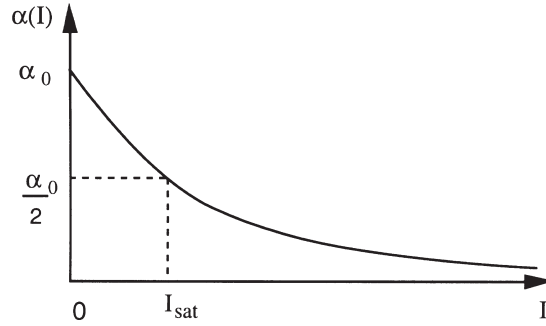


Fig. 2.20. Simple hyperbolic model of the absorption coefficient α of a two-level system versus incident intensity. When the intensity reaches the saturation value I_{sat} the low-intensity absorption α_0 is reduced by a factor of two

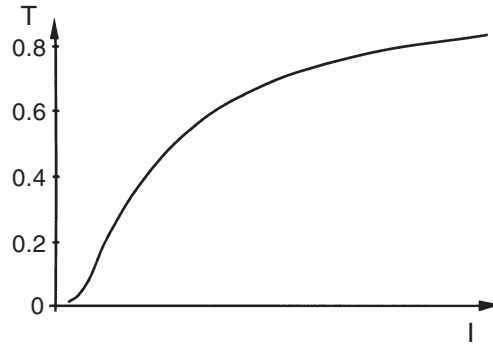


Fig. 2.21. Numerical simulation of transmission versus incoming intensity in a two-level electronic system

Saturable absorbers can be split into two classes depending on the speed of the change of transmission. Fast saturable absorbers have an instantaneous response under light illumination. Figure 2.22 shows a simulation of the effect of such a saturable absorber on a Gaussian pulse.

On the wings of the pulse, where the intensity is low, absorption takes place, while the summit of the pulse remains mostly unchanged. As a result of its propagation through the fast saturable absorber the pulse undergoes a temporal narrowing.

Saturation in a slow saturable absorber depends on the light intensity integrated over some characteristic time duration. As a result, the leading part of the pulse is strongly absorbed. Once saturation is reached, the saturation of the absorption decays with some other characteristic time and the trailing part of the pulse passes through the medium with no distortion. The result of the nonlinear absorption is asymmetric, as can be seen in Fig. 2.23.

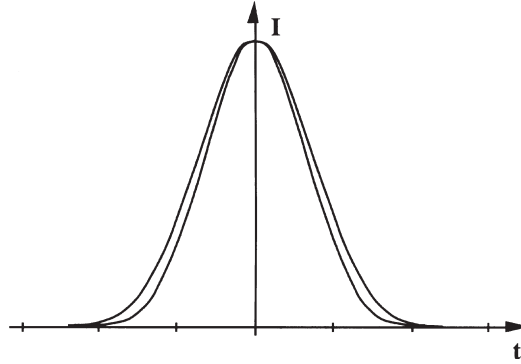


Fig. 2.22. Numerical simulation of the effect of a fast saturable absorber on a Gaussian light pulse. In order to make clear the narrowing of the pulsation of the pulse, the modified pulse has been normalized to the original one

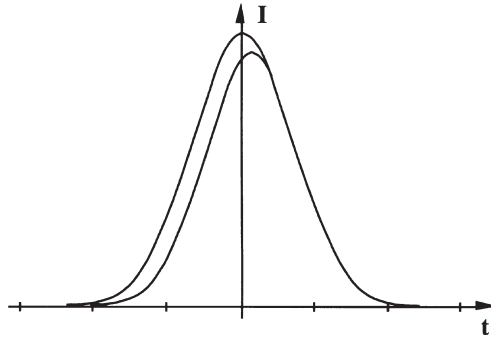


Fig. 2.23. Numerical simulation of the effect of a slow saturable absorber on a Gaussian light pulse

“Slow” and “fast” only have a meaning when comparing the characteristic time of the saturable absorber with the duration of the light pulses. For ultrashort light pulses, say less than a few picoseconds, all saturable absorbers are slow ones.

In a simple description, the photons from the leading part of a light pulse penetrating a saturable absorber disappear when promoting electrons from a ground to an excited state. As the pulse propagates further, more and more photons are absorbed, promoting more and more electrons, up to the point at which the ground-state and excited electronic populations are equalized (see Chap. 1) and no more absorption can take place. The dynamics of the saturation are under the control of the electronic relaxations.

2.4 Cascaded Nonlinearities

Cascading effects were discovered in 1986 when U. Osterberg and W. Margulis [2.1] observed the doubling of a Nd:YAG laser beam in a centrally symmetric optical fibre with a 10% yield. They had, however, been discovered in 1972 by E. Yablanovitch, C. Flytzanis, and N. Bloembergen [2.2]. The electric field E which appears in the development of the material polarization (expression (2.1)) is the total macroscopic field and, as the polarization modifies the field through Maxwell's equations, it is an unknown quantity. In the development of the optical nonlinearities we have considered so far, the effect of the medium polarization on the field in the medium was not considered: only the contribution $E^{(1)}$ to the field that would occur if the medium would have a linear response was taken into account. The total response of a material to an applied electric field is therefore a nonlinear function of this $E^{(1)}$ field, and it contains products of the nonlinear susceptibilities $\chi^{(i)}$. These terms are referred to as cascaded nonlinearities.

No cascading effect has to be considered including the linear susceptibility $\chi^{(1)}$ because this term depends only on the linear field. Therefore the lowest-order cascading term contains $\chi^{(2)}.\chi^{(2)}$ a fourth-order rank tensor which is therefore equivalent to a direct $\chi^{(3)}$ third-order optical nonlinearity.

To exemplify a cascading process we will examine the third-harmonic generation in a material with no central symmetry. For the sake of simplicity, scalar susceptibilities and no polarizations of the field will be considered. We start with the linear field $E^{(1)} = E_\omega = A_\omega e^{ik_\omega x}$ being a plane wave propagating in the x direction. This wave induces a material polarization at pulsation 2ω

$$P_{2\omega} = \frac{\varepsilon_0}{2} \chi^{(2)} E_\omega E_\omega, \quad (2.60)$$

as well as a polarization at pulsation 3ω

$$P_{3\omega} = \frac{\varepsilon_0}{4} \chi^{(3)} E_\omega E_\omega E_\omega. \quad (2.61)$$

The second-order polarization induces a second harmonic field

$$E_{2\omega} = A_{2\omega} e^{ik_{2\omega} x}, \quad (2.62)$$

which amplitude can be calculated in the nondepletive regime, when the decrease of the fundamental amplitude is negligible, from the light propagation equation

$$E_{2\omega} = \frac{\omega}{2n_{2\omega}c} \chi^{(2)} \frac{1}{\Delta k} (1 - e^{-i\Delta k x}) E_\omega E_\omega \quad (2.63)$$

where $n_{2\omega}$ is the index of refraction of light at the two-photon pulsation, and

$$\Delta k = 2k_\omega - k_{2\omega} = \frac{2\omega}{c} (n_\omega - n_{2\omega}) \quad (2.64)$$

is the phase mismatch between the fundamental and the doubled waves. The generated second harmonic wave mixes with the fundamental wave through up-conversion (sum-frequency generation)

$$P'_{3\omega} = \varepsilon_0 \chi^{(2)} E_{2\omega} E_{\omega}, \quad (2.65)$$

which by using equation (2.63) leads to the following cascading contribution:

$$P'_{3\omega} = \varepsilon_0 \frac{\omega}{2n_{2\omega}c} \chi^{(2)} \chi^{(2)} \frac{1}{\Delta k} (1 - e^{-i\Delta k x}) E_{\omega} E_{\omega} E_{\omega} \quad (2.66)$$

so that the real material polarization at the third harmonic pulsation contains a term depending on $\chi^{(2)} \chi^{(2)}$. In this simplified model the cascaded third-order polarization diverges when the phase-matching condition for the second-harmonic generation $\Delta k = 0$ is realised so that it becomes the main contribution to the third harmonic generation. The enlarged third-order susceptibility is written as:

$$\chi_t^{(3)} = \chi^{(3)} + \frac{\omega}{2n_{2\omega}c} \chi^{(2)} \chi^{(2)} \frac{1}{\Delta k} (1 - e^{-i\Delta k x}), \quad (2.67)$$

which depends on the propagation length x . In the case when phase matching is realized for the pure third harmonic generation process (first contribution in Eq. (2.67)) the phase-matching condition for the second harmonic generation process is not fulfilled and the exponential term in (2.67) becomes negligible and the expression simplifies to

$$\chi_t^{(3)} = \chi^{(3)} + \frac{\omega}{2n_{2\omega}c\Delta k} \chi^{(2)} \chi^{(2)}, \quad (2.68)$$

which is now independent of the length of propagation.

The simple appearance of the effect as described earlier is deceptive because cascading effects are vector dependent, they vary with the propagation vectors of the light beams as well as with their polarization. They cannot always be distinguished from the direct-order nonlinear effects and their amplitude is generally of the same order of magnitude. Generally, an n th-order polarization has contributions arising from any set $\{n_i\}$ of multistep processes such that $\sum_i (n_i - 1) = n - 1$. General solutions for the optical cascading equations describing the $\chi^{(2)} : \chi^{(2)}$ process have been developed in reference [2.3].

The frequency doubling in a fibre mentioned in the introduction was tricky. It was shown that, because of surface symmetry breaking, a small amount of doubled frequency is created at the entrance of the fibre. The interference between the rectified field from the fundamental and doubled frequencies creates a static grating that in turn creates and organises macroscopic dipoles owed to the presence of doping atoms in the fibre (the original experiments were performed in germanium-doped fibres). This optical polling of the fibre breaks down the central symmetry and efficient frequency doubling can take place [2.4].

Considerable energy has been spent developing the cascaded Kerr with the perspective of developing optronic devices [2.5]. Non-phase-matched second harmonic is generated in a fibre that is down-converted to the fundamental frequency because of the non-phase-matched case. Then the phase shift between the fundamental light and the down-converted one translates as an intensity-dependent index change equivalent to a classical Kerr effect.

Cascading has been recognised as a way to efficiently generate fourth harmonic [2.6] of optical spatiotemporal solitons [2.7]; quantum optics should rapidly benefit from the recent advances of the field.

2.5 Problems

1. A light pulse has an intensity envelope shaped as a Gaussian function $I(t) = \exp(t/t_0)^2$. Calculate the full width at half maximum Δt (FWHM) for this pulse.

The autocorrelation function of the pulse envelope can be measured and is expressed as $G(\tau) = \int_{-\infty}^{+\infty} I(t)I(t-\tau) dt$. Explicitly calculate the autocorrelation function of the pulse.

What is the FWHM $\Delta t'$ of this pulse autocorrelation function? What is the value of the ratio $\Delta t'/\Delta t$? (Answer: $\sqrt{2}$)

2. Coherence length for frequency doubling in a quartz crystal.

For quartz, the ordinary index n_o is isotropic. In a plane which contains the \mathbf{c} axis and the propagation direction \mathbf{k} , the ordinary index lies on a circle with radius n_o . In that same plane the extraordinary index lies on an ellipse described by $[1/n_e(\theta)]^2 = \cos^2 \theta/n_o^2 + \sin^2 \theta/n_e^2$, θ being the angle between \mathbf{c} and \mathbf{k} .

Consider a fundamental wavelength in vacuum $\lambda_0^{(1)} = 620 \text{ nm}$ and its doubled counterpart $\lambda_0^{(2)} = 310 \text{ nm}$; the indices for quartz close to these wavelengths are given in the following table:

$\lambda (\mu\text{m})$	n_o	n_e
0.62782	1.542819	1.551880
0.312279	1.57433	1.584485

Show that under these circumstances there is no crossing between the index curves for the fundamental and doubled frequencies. Phase matching is not possible in quartz, at least for these wavelengths.

From 2.43 it can be used that $I(2\omega) \propto \sin^2 \Delta k L/2$, L being the thickness of the crystal. This expression shows that the length $L_c = 2\pi/\Delta k$, called the coherence length, maximizes the intensity of the doubled frequency. Assuming type I propagation in a quartz crystal of a single beam with central wavelength 620 nm, the phase mismatch can be written as

$$\Delta k = k_e^{2\omega} - 2k_o^\omega \quad \text{and} \quad k = 2\pi n(\lambda_0)/\lambda_0. \quad (2.69)$$

What is the value of the coherence length when the beam propagates along the c axes, $\theta = 0$? Using your favored mathematics software, plot the dependence of the coherence length on θ , under these conditions.

3. Show that the pulsation chirp law described by expression (2.16)

$$\omega(t) = \partial\phi/\partial t = \omega_0 + at$$

is a limit when the observation time t is smaller than the duration of the pulse ($\Gamma t^2 \ll 1$). Deduce the value of the parameter a . (Answer: $a = \omega_0 n_2 x \Gamma / c$).

Further Reading

- S.A. Akhmanov, V.A. Vysloukh, A.S. Chirkin: *Optics of Femtosecond Laser Pulses* (American Institute of Physics, New York 1992)
 R.R. Alfano (ed.): *The Supercontinuum Laser Source* (Springer, Berlin, Heidelberg 1989)
 M. Born, E. Wolf: *Principles of Optics* (Pergamon, Oxford 1993)
 H. Haken: *Light*, Vol. 1, "Waves, photons, atoms" (North-Holland, Amsterdam 1986)
 J.D. Jackson: *Classical Electrodynamics*, 2nd edn. (Wiley, New York 1974)
 L. Landau, E. Lifschitz: *Field Theory* (Mir, Moscow 1966)
 S.L. Shapiro (ed.): *Ultrashort Light Pulses*, Topics in Applied Physics, Vol. 18 (Springer, Berlin, Heidelberg 1977)
 A.E. Siegman: *Lasers* (University Science Books, Mill Valley, CA 1986)
 A. Yariv: *Quantum Electronics*, 3rd edn. (Wiley, New York 1989)

References

- [2.1] U. Osterberg, W. Margulis: *Optics Lett.* **11**, 516 (1986)
 [2.2] E. Yablanovitch, C. Flyzanis, N. Bloembergen: *Phys. Lett.* **29**, 865 (1972)
 [2.3] S. Lafortune, P. Winternitz, C.R. Menyuk: *Phys. Rev. E.*, **58**, 2518 (1998)
 [2.4] B.P. Antonyuk: *V.B. Antonyuk Physics-Uspekhi*, **44**, 53 (2001)
 [2.5] R. Schiek: *J. Opt. Soc. Am.* **10**, 1848 (1993)
 [2.6] A.A. Sukhorukov, T.J. Alexander, Y.S. Kivshar, S.M. Saltiel: *Phys. Lett. A*, **281**, 34 (2001)
 [2.7] M. de Sterke, S.M. Saltiel, Y.S. Kivshar: *Opt. Lett.*, **26**, 539 (2001)
 [2.8] X. Liu, L.J. Qian, F.W. Wise: *Phys. Rev. Lett.*, **82**, 4631 (1999)



<http://www.springer.com/978-0-387-01769-3>

Femtosecond Laser Pulses
Principles and Experiments
Rulliere, C. (Ed.)
2005, XVI, 426 p., Hardcover
ISBN: 978-0-387-01769-3